

Predictions of m_{ee} and neutrino mass from a consistent Froggatt-Nielsen model

Yu-Cheng Qiu,^{1,*} Jin-Wei Wang,^{2,†} and Tsutomu T. Yanagida^{1,3,‡}

¹*Tsung-Dao Lee Institute and School of Physics and Astronomy,
Shanghai Jiao Tong University, 520 Shengrong Road, Shanghai, 201210, China*

²*School of Physics, University of Electronic Science and Technology of China, Chengdu 611731, China*

³*Kavli IPMU (WPI), The University of Tokyo, Kashiwa, Chiba 277-8583, Japan*

The seesaw mechanism is the most attractive mechanism to explain the small neutrino masses, which predicts the neutrinoless double beta decay ($0\nu\beta\beta$) of the nucleus. Thus the discovery of $0\nu\beta\beta$ is extremely important for future particle physics. However, the present data on the neutrino oscillation is not sufficient to predict the value of m_{ee} as well as the neutrino mass m_ν^i . In this short article, by adopting a simple and consistent Froggatt-Nielsen model, which can well explain the observed masses and mixing angles of quark and lepton sectors, we calculate the distribution of m_{ee} and m_ν^i . Interestingly, a relatively large part of the preferred parameter space can be detected in the near future.

I. INTRODUCTION

The Standard Model of particle physics contains 28 free parameters, including the neutrino sector, which could not be explained theoretically. Among them, Yukawa couplings have a hierarchy structure, that is the flavor puzzle, which has attracted theorists' attention for decades [1–8]. Meanwhile, for the neutrino sector, the neutrino oscillation experiments, e.g. Super-K [9], SNO [10], and Daya Bay [11], have shown that neutrinos are not massless but possess tiny mass m_ν^i ($i = 1, 2, 3$). Among different explanations, the seesaw mechanism [12–15] is regarded as the most natural and promising one. An important corollary to the seesaw mechanism is the neutrinoless double beta decay ($0\nu\beta\beta$), which is closely related to the effective Majorana mass m_{ee} . Therefore, the discovery of $0\nu\beta\beta$ will be a huge breakthrough for the particle physics community. Nevertheless, neither the seesaw mechanism nor neutrino oscillation experiments can tell the values of m_{ee} and m_ν^i . This could be viewed as another intriguing puzzle. In this work, we try to propose a simple and consistent model that can well explain the fermion mass hierarchy and predict the values of m_{ee} and m_ν^i simultaneously.

It is well known that the Froggatt-Nielsen (FN) mechanism [16–18] provides an excellent method to explain the flavor puzzle, in which the Standard Model (SM) gauge group is extended by a horizontal global $U(1)_{\text{FN}}$ symmetry. The $U(1)_{\text{FN}}$ is broken by a vacuum expectation value (VEV) of a new scalar field ϕ whose $U(1)_{\text{FN}}$ charge is -1 . Naturally, a dimensionless parameter λ can be defined, i.e. $\lambda = \langle\phi\rangle/M_{\text{PL}} \sim \mathcal{O}(0.1)$, where $M_{\text{PL}} \simeq 2.4 \times 10^{18}$ GeV is the reduced Planck scale. All SM particles also carry the $U(1)_{\text{FN}}$ charge, and the value of the FN charge is generation dependent, which indicates that the masses of different generations of particles get suppressed by different powers of λ . Thus, the hierarchy issue could be well

explained by the FN mechanism (see Ref. [8] for a very recent review).

Obviously, the core of the FN mechanism is the assignment of FN charge for SM particles. Recently, there are some works that did a blanket search to find optimal FN charge assignment [19, 20]. Especially, in Ref. [19] the advanced reinforcement learning technics are involved. In our work, instead of adopting these kinds of brute force methods, we attempt to fix the FN charge of SM particles by doing a qualitative analysis. The rationality of the FN charge assignment is evaluated by comparing the theory predictions with experimental observations. In fact, it turns out that our strategy is quite effective, and to some extent, our results are in good agreement with previous blanket scan results [20].

As for the more interesting neutrino sector, the seesaw mechanism actually implies that the neutrino masses can be produced from a dimension-five effective operator [14, 21, 22], which can be derived by integrating out the heavy right-handed neutrino states. In this case, the neutrino mass and mixing angle are also affected by the FN charge, since ν_L^i belongs to the electroweak doublet ℓ_L^i and also carries FN charges. Therefore, we show that it is possible to handle the flavor and neutrino puzzle within a unified FN framework. Interestingly, combined with the measurements of neutrino mass square difference Δm_{21}^2 , $|\Delta m_{32}^2|$ [23], and some cosmological constraints on $\sum m_\nu^i$ [24], we can calculate the distribution of m_{ee} and m_ν^i . Surprisingly, we find that our predictions on m_ν^i are quite consistent with the available experimental data. Besides, a relatively large parameter space of m_{ee} of our model could be explored in the near future neutrinoless $\beta\beta$ decay experiment, e.g. LEGEND-1000 [25].

This paper is organized as follows. In Sec. II we give a brief introduction to the FN mechanism and the analysis of how to fix the FN charges. In Sec. III we calculate the predictions of our model on m_{ee} and m_ν^i as well as the near future constraints from LEGEND-1000. Conclusions and further discussions are given in Sec. IV.

* ethanqiu@sjtu.edu.cn

† jinwei.wang@uestc.edu.cn

‡ tsutomu.tyanagida@sjtu.edu.cn

II. THE CONSISTENT FORGGATT-NIELSEN MODEL

The FN model we are considering is a simple extension of the Standard Model [16–18]. The mass matrices of quarks are granted by Yukawa couplings, which are

$$-\mathcal{L} \supset y_u^{ij} \bar{Q}_L^i \tilde{H} u_R^j + y_d^{ij} \bar{Q}_L^i H d_R^j + \text{h.c.}, \quad (1)$$

where H is the Standard Model Higgs doublet and $\tilde{H} = i\sigma_2 H^*$. Under our FN framework, the Yukawa couplings can be expressed as

$$y_u^{ij} = g_{ij} \lambda^{n_u^{ij}}, \quad y_d^{ij} = g_{ij} \mathcal{N} \lambda^{n_d^{ij}}, \quad (2)$$

where the \mathcal{N} is an overall factor to accommodate the overall scale difference between up-type and down-type sectors, whose origin could be two-Higgs-doublet models at high energy [26], the g_{ij} is the universal coupling, whose magnitude $|g_{ij}|$ fulfills a normal distribution $N(\mu, \sigma^2)$, while its argument fulfills a uniform distribution from 0 to 2π . In our work, we choose $\mu = 1$ and $\sigma = 0.3$ for a benchmark case. Since we have set $U(1)_{\text{FN}}^H = 0$ and $U(1)_{\text{FN}}^\phi = -1$, the value of $n_{u/d}^{ij}$ is determined by the FN charge of quarks,

$$n_u^{ij} = U(1)_{\text{FN}}^{\bar{Q}_L^i} + U(1)_{\text{FN}}^{u_R^j}, \quad (3a)$$

$$n_d^{ij} = U(1)_{\text{FN}}^{\bar{Q}_L^i} + U(1)_{\text{FN}}^{d_R^j}. \quad (3b)$$

Clearly, once we fix the value of λ and quarks' FN charge, the quark mass, mixing angle, and CP angle are almost fixed. Mass hierarchy is indicated by the fermion mass ratio between generations, i.e. m_u/m_t , m_d/m_b , and so on. We find that if we focus on the mass ratios, then the charge assignment will become much easier. Take \bar{Q}_L^i and d_R^j for example, where the most general form of their FN charge should be $U(1)_{\text{FN}}^{\bar{Q}_L^i} = \{a, b, c\}$ and $U(1)_{\text{FN}}^{d_R^j} = \{d, e, f\}$, then we have

$$\lambda^{n_d^{ij}} = \lambda^{c+f} \begin{pmatrix} \lambda^{a-c+d-f} & \lambda^{a-c+e-f} & \lambda^{a-c} \\ \lambda^{b-c+d-f} & \lambda^{b-c+e-f} & \lambda^{b-c} \\ \lambda^{d-f} & \lambda^{e-f} & 1 \end{pmatrix}. \quad (4)$$

The overall factor λ^{c+f} will not affect the fermion mass ratio and mixings. However, this factor could also be used to explain the absolute quark mass (such as \mathcal{N} in Eq. (1)), i.e. the mass hierarchy between up-type and down-type quarks. In the following content, we just set the FN charge of third-generation fermion equal to zero, which is equivalent to absorbing the λ^{c+f} factor into \mathcal{N} , and we will comment on this issue in Sec. IV. For simplicity, we only consider the FN charge to be an integer or half-integer less than 5. Similar conditions are also adopted in previous literature [19, 20].

For the quark sector, one could show that the Cabibbo-Kobayashi-Maskawa (CKM) matrix is mainly determined

TABLE I. Experimental measured quantities. Quark and lepton mass ratios are taken at the scale of 10^{12} GeV [29], which are almost energy scale independent [30]. Mixing angles and CP phases are in the rad unit [31].

m_u/m_t	m_c/m_t	m_d/m_b	m_s/m_b
6.58×10^{-6}	0.00333	0.00104	0.0201
θ_{12}^C	θ_{23}^C	θ_{13}^C	δ^C
0.227	0.0418	0.00369	1.14
m_e/m_τ	m_μ/m_τ	$\Delta m_{21}^2/\Delta m_{32}^2$	
0.000279	0.0589	0.0307	
θ_{12}^P	θ_{23}^P	θ_{13}^P	δ^P
0.591	0.844	0.150	$-2.41_{-0.489}^{+0.663}$

by the \bar{Q}_L^i . The well-known Wolfenstein parametrization [27] indicates that mixing angles in the CKM matrix approximately satisfy $\sin \theta_{12}^C \sim \lambda'$, $\sin \theta_{23}^C \sim \lambda'^2$ and $\sin \theta_{13}^C \sim \lambda'^3$, where $\lambda' \sim 0.2$. It is attempted to assume that $\lambda \sim \mathcal{O}(\lambda')$, and the FN charge of the quark doublet shall be $U(1)_{\text{FN}}^{\bar{Q}_L^i} = \{3, 2, 0\}$ to produce such a mixing pattern [20, 28]. Once we know the $U(1)_{\text{FN}}^{\bar{Q}_L^i}$, the FN charge of u_R and d_R can be roughly fixed by comparing with the observed quark mass ratios.

In Table I we have summarized all available mass ratios, mixing angles, and CP angles of quark and lepton sectors. Considering that the $U(1)_{\text{FN}}$ was broken at a very high energy scale $\sim M_{\text{PL}}$, all the numbers in Table I should also be evaluated at a high energy scale. From Refs. [29, 30], we can see that the mass ratio of the quark and lepton sectors are almost energy independent as long as the energy scale larger than $\sim 10^8$ GeV. Therefore, we can safely substitute the mass ratio at $\sim 10^{12}$ GeV for the results at $\sim M_{\text{PL}}$. As for the mixing angles and CP angle, we assume that they are energy independent.

Assuming the FN charges of u_R and d_R are $\{a, b, 0\}$ and $\{c, d, 0\}$, respectively, we can derive that

$$n_u = \begin{pmatrix} 3+a & 3+b & 3 \\ 2+a & 2+b & 2 \\ a & b & 0 \end{pmatrix}, \quad n_d = \begin{pmatrix} 3+c & 3+d & 3 \\ 2+c & 2+d & 2 \\ c & d & 0 \end{pmatrix}. \quad (5)$$

From Table I we roughly have

$$\frac{m_u}{m_t} \sim \lambda'^7, \quad \frac{m_c}{m_t} \sim \lambda'^{3.5}, \quad \frac{m_d}{m_b} \sim \lambda'^4, \quad \frac{m_s}{m_b} \sim \lambda'^2, \quad (6)$$

where the $\lambda' \sim 0.2$. Comparing Eq. (5) and Eq. (6), we can derive that

$$a = 4, \quad b = 1.5, \quad c = 1, \quad d = 0. \quad (7)$$

For the lepton sector, the mass terms are generated by Yukawa couplings and a five-dimensional operator, that is

$$-\mathcal{L} \supset y_\ell^{ij} \bar{\ell}_L^i H e_R^j + \frac{1}{M} y_\nu^{ij} \left(\bar{\ell}_L^i \tilde{H}^* \right) \left(\tilde{H}^\dagger \ell_L^j \right) + \text{h.c.}, \quad (8)$$

TABLE II. FN charge of quarks and leptons.

Generation i	1	2	3
\bar{Q}_L	3	2	0
u_R	4	1.5	0
d_R	1	0	0
$\bar{\ell}_L$	1	0.5	0
e_R	4	1	0

where

$$y_\ell^{ij} = g_{ij} \mathcal{N} \lambda^{n_\ell^{ij}}, \quad y_\nu^{ij} = g'_{ij} \lambda^{n_\nu^{ij}}. \quad (9)$$

Note that here we use the same \mathcal{N} as Eq. (2) because of the fact that $m_b \sim m_\tau$ at a very high energy scale [29]. Besides, the g'_{ij} is a symmetric matrix due to the Majorana nature of the neutrino. Similar to the quark sector, the Pontecorvo-Maki-Nakagawa-Sakata (PMNS) matrix is mainly determined by $\bar{\ell}_L^i$. The observations tell us that the mixing angles θ_{12}^P and θ_{23}^P are relatively larger compared to θ_{13}^P , and θ_{12}^P is slightly smaller than θ_{23}^P . Following a similar logic and using the universal λ' , we assign the FN charge for the lepton doublet as $U(1)_{\bar{\ell}_L}^{\text{FN}} = \{1, 0.5, 0\}$. One interesting fact is that we can easily prove that the rank of n_ν is 1, which means there would be two mass eigenvalues being almost zero and one relatively large eigenvalue after diagonalization. This indicates that the FN mechanism naturally prefers normal order (NO)¹. Therefore, in the following content, we just stick to the NO scenario.

Then $U(1)_{\text{FN}}^{\text{eR}}$ is obtained from estimating the charged lepton mass ratios. Specifically, assuming $U(1)_{\text{FN}}^{\text{eR}} = \{e, f, 0\}$ we have

$$n_\ell = \begin{pmatrix} 1+e & 1+f & 1 \\ 0.5+e & 0.5+f & 0.5 \\ e & f & 0 \end{pmatrix}. \quad (10)$$

From Table. I we roughly have

$$\frac{m_e}{m_\tau} \sim \lambda^5, \quad \frac{m_\mu}{m_\tau} \sim \lambda^{1.5}, \quad (11)$$

where the $\lambda' \sim 0.2$. Comparing Eq. (10) and Eq. (11), we can derive that

$$e = 4, \quad f = 1. \quad (12)$$

Until now, by doing a qualitative analysis we have fixed the FN charge of SM particles (see Table II). However, there are two issues that need to be emphasized. The

¹ Another perspective to understand this feature is through the FN charge assignment of $\bar{\ell}_L$. Combining Eq. (8) and $U(1)_{\bar{\ell}_L}^{\text{FN}} = \{1, 0.5, 0\}$ (see Table II), the ratio of three eigenvalues of y_ν^{ij} is roughly $1 : \lambda' : \lambda'^2$, which is clearly NO for $\lambda' \sim 0.2$.

first one is the global $U(1)_{\text{FN}}$ symmetry. The above analysis is based on an assumption that all terms in Eq. (1) and Eq. (8) respect the global $U(1)_{\text{FN}}$. However, it is believed that any global symmetries must be broken by non-perturbation effects in quantum gravity [32]. With the charge assignment in Table II, we found there is a discrete \mathbf{Z}_{33} symmetry, actually this symmetry is anomaly-free for $\mathbf{Z}_{33} \times [SU(2)_L]^2$ and $\mathbf{Z}_{33} \times [SU(3)_c]^2$, and therefore can be gauged. This can be regarded as quite an interesting feature of our model.

Another issue is the exact value of λ , which is the only free parameter after fixing the FN charge. We conduct the analysis by using a very rough number, i.e. $\lambda \sim \lambda' \sim 0.2$, while a more accurate λ is necessary for a concrete FN model. In the following content, we adopt the minimum chi-square method to find the best value of λ .

The strategy is quite straightforward. As we mentioned above, in our model the g_{ij} is the universal coupling whose magnitude fulfills a normal distribution $N(1, 0.3)$, while its argument fulfills a uniform distribution from 0 to 2π . With the fixed FN charges and λ , all the couplings, e.g., y_u^{ij} , y_d^{ij} , y_ℓ^{ij} , y_ν^{ij} , can be generated. Then, all the desired quantities (denoted X_i), including the quark and lepton mass ratios, the mixing angles, and CP angles, will be fixed. By randomly generating g_{ij} we can derive the distribution X_i . The chi square is defined as

$$\chi^2(\lambda) = \sum_i \left(\frac{E(X_i) - X_i^{\text{exp}}}{\sqrt{V(X_i)}} \right)^2, \quad (13)$$

where X_i^{exp} is the experimentally measured value (see Table I), $E(X_i)$ is the expectation value of X_i , while $V(X_i)$ is the deviation. Here we take

$$X_i \in \left\{ \frac{m_u}{m_t}, \frac{m_c}{m_t}, \frac{m_d}{m_b}, \frac{m_s}{m_b}, \frac{m_e}{m_\tau}, \frac{m_\mu}{m_\tau}, \frac{\Delta m_{21}^2}{\Delta m_{32}^2}, \theta_{12}^C, \theta_{23}^C, \theta_{13}^C, \delta^C, \theta_{12}^P, \theta_{23}^P, \theta_{13}^P \right\},$$

where δ^P is not the direct observable. By scanning the parameter space of λ we can find the best value that minimizes the $\chi^2(\lambda)$.

To calculate Eq. (13) we need the exact distribution of X_i . For the quark sector, the Yukawa matrices can be decomposed as

$$y_u = U_u D_u W_u^\dagger, \quad y_d = U_d D_d W_d^\dagger, \quad (14)$$

where $U_{u,d}$ and $W_{u,d}$ are unitary matrices, $D_{u,d}$ is a diagonal matrix with all real elements. The U_u and W_u are obtained from $y_u y_u^\dagger = U_u (D_u)^2 U_u^\dagger$ and $y_u^\dagger y_u = W_u (D_u)^2 W_u^\dagger$, and the same is true for the U_d and W_d . Then up-type and down-type quark mass ratios are

$$\begin{aligned} \frac{m_u}{m_t} &= \frac{D_u^{11}}{D_u^{33}}, & \frac{m_c}{m_t} &= \frac{D_u^{22}}{D_u^{33}}, \\ \frac{m_d}{m_b} &= \frac{D_d^{11}}{D_d^{33}}, & \frac{m_s}{m_b} &= \frac{D_d^{22}}{D_d^{33}}. \end{aligned} \quad (15)$$

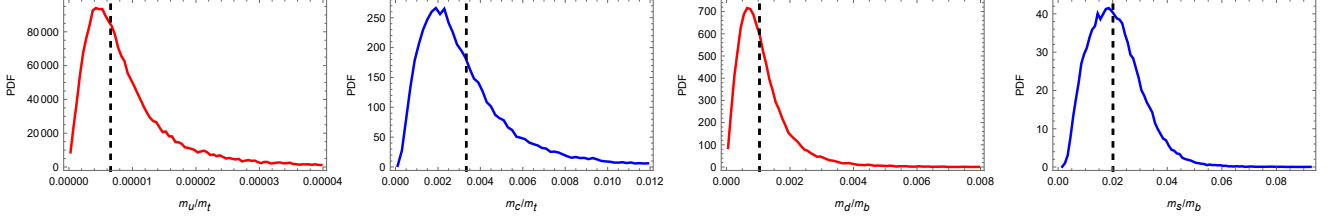


FIG. 1. The PDF of quark mass ratios with $\lambda = 0.171$ and $\sigma = 0.3$. The black dashed vertical lines indicate the experimental measurements given in Table I.

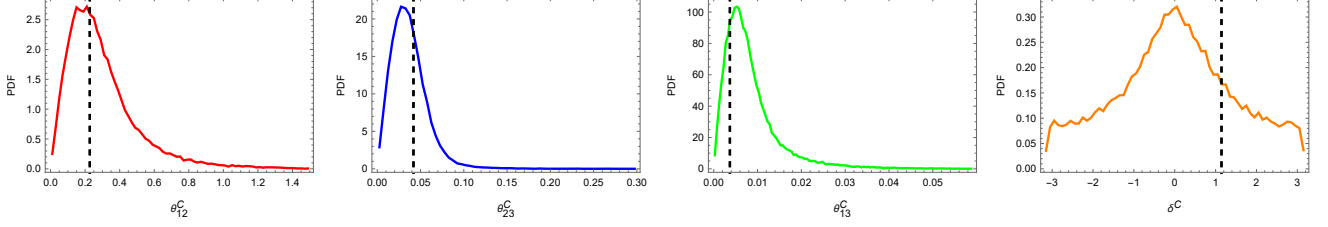


FIG. 2. The PDFs of the mixing angle θ_{ij}^C and CP angle δ^C of quark sector with $\lambda = 0.171$ and $\sigma = 0.3$. The black dashed vertical lines indicate the experimentally measured value as indicated in Table I.

Within our notation, the CKM matrix can be expressed as

$$U_{\text{CKM}} = U_u^\dagger U_d, \quad (16)$$

which contains all information on quark mixing angles (θ_{ij}^C) and CP angle (δ^C). Under standard parametriza-

tion, the U_{CKM} is

$$U_{\text{CKM}} = V_{\text{SP}}(\theta_{12}^C, \theta_{23}^C, \theta_{13}^C, \delta^C), \quad (17)$$

where V_{SP} is a unitary matrix possessing four real parameters, that is

$$V_{\text{SP}}(\theta_{12}, \theta_{23}, \theta_{13}, \delta) = \begin{pmatrix} c_{13}c_{12} & c_{13}s_{12} & s_{13}e^{-i\delta} \\ -c_{23}s_{12} - s_{23}s_{13}c_{12}e^{i\delta} & c_{23}c_{12} - s_{23}s_{13}s_{12}e^{i\delta} & s_{23}c_{13} \\ s_{23}s_{12} - c_{23}s_{13}c_{12}e^{i\delta} & -s_{23}c_{12} - c_{23}s_{13}s_{12}e^{i\delta} & c_{23}c_{13} \end{pmatrix}, \quad (18)$$

where $c_{ij} = \cos \theta_{ij}$ and $s_{ij} = \sin \theta_{ij}$. Note that we adopt the convention that $\theta_{ij} \in [0, \pi/2)$ and $\delta \in [-\pi, \pi)$. Utilizing Eq. (15) and Eq. (18), we can calculate quark sector parameters.

One significant difference for the lepton sector (see Eq. (8)) is that the neutrino mass is generated by a five-dimensional effective operator. As we mentioned in this case y_ν is a complex symmetric matrix. Similar to the quark sector, we do the following decomposition, i.e.,

$$y_\ell = U_\ell D_\ell W_\ell^\dagger, \quad y_\nu = U_\nu D_\nu U_\nu^T, \quad (19)$$

where D_ℓ and D_ν are diagonal matrices with all real elements and U_ℓ , W_ℓ , and U_ν are unitary matrices. The U_ℓ and W_ℓ are obtained from $y_\ell y_\ell^\dagger = U_\ell (D_\ell)^2 U_\ell^\dagger$ and $y_\ell^\dagger y_\ell = W_\ell (D_\ell)^2 W_\ell^\dagger$. Then the mass ratios for charged

leptons are

$$\frac{m_e}{m_\tau} = \frac{D_\ell^{11}}{D_\ell^{33}}, \quad \frac{m_\mu}{m_\tau} = \frac{D_\ell^{22}}{D_\ell^{33}}. \quad (20)$$

Next, we need to derive the explicit form of U_ν . Define \tilde{U}_ν such that $y_\nu^\dagger y_\nu = \tilde{U}_\nu (D_\nu)^2 \tilde{U}_\nu^\dagger$, and since y_ν is a symmetric matrix, we can derive that $y_\nu = \tilde{U}_\nu \Phi D_\nu \tilde{U}_\nu^T$, where Φ is a diagonal matrix and each element is a pure phase. Compared with Eq. (19) we have $U_\nu = \tilde{U}_\nu \Phi^{-1/2}$. In our notation, the PMNS matrix can be written as

$$U_{\text{PMNS}} = U_\ell^\dagger U_\nu^*, \quad (21)$$

Different from the CKM matrix, one could only rotate three phases from charged leptons, which results in two

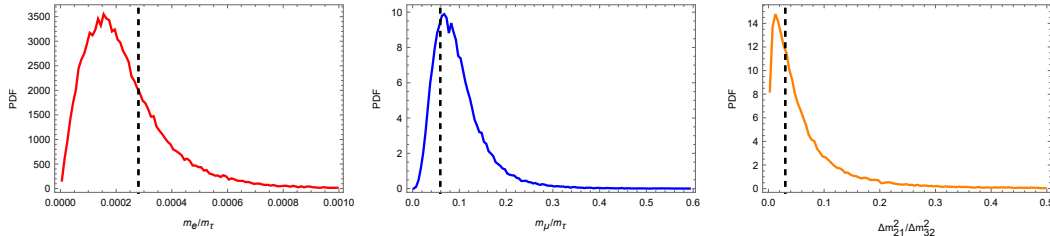


FIG. 3. Similar to Fig. 1 but the lepton sector. Note that for neutrinos the ratio of mass square difference, i.e., $\Delta m_{21}^2/\Delta m_{32}^2$ is shown.

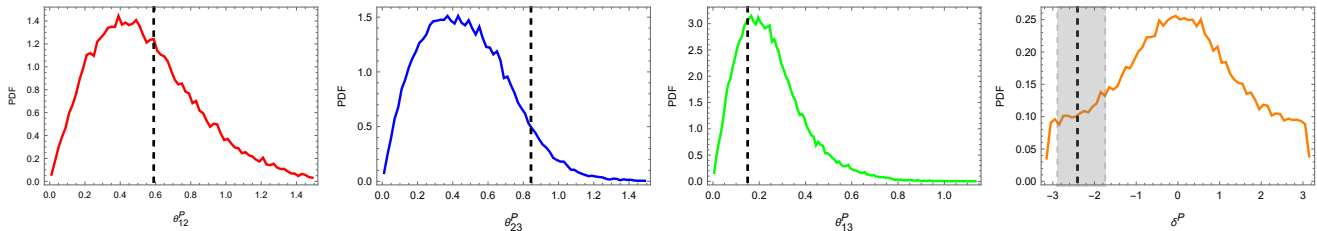


FIG. 4. Similar to Fig. 2 but for the neutrino sector. The Gray dashed vertical lines indicate the experimentally measured values as indicated in Table I.

extra phases in U_{PMNS} compared to the CKM matrix,

$$U_{\text{PMNS}} = V_{\text{SP}}(\theta_{12}^{\text{P}}, \theta_{23}^{\text{P}}, \theta_{13}^{\text{P}}, \delta^{\text{P}}) \begin{pmatrix} 1 & 0 & 0 \\ 0 & e^{i\frac{\alpha_{\text{M}}}{2}} & 0 \\ 0 & 0 & e^{i\frac{\beta_{\text{M}}}{2}} \end{pmatrix}, \quad (22)$$

where α_{M} and β_{M} are the Majorana phases. In our work, we only consider θ_{ij}^{P} and δ^{P} .

So now we know how to calculate X_i , and then by repeating random sampling g_{ij} and g'_{ij} , we can get the distribution of X_i . Combining with Eq. (13) we do a parameter scan to get the best value of λ , that is

$$\lambda = 0.171 \quad \text{with} \quad \chi^2 = 4.69. \quad (23)$$

Under such an input, the probability density function (PDF) of the quark mass ratios are plotted in Fig. 1, and the results of mixing angles and CP angle are shown in Fig. 2. The black dashed lines indicate the experimental measurements (see Table I). It shows that our model predictions all agree with the experimental observations. Similarly, Fig. 3 and Fig. 4 show the PDF of the lepton mass ratio and mixing angles. For neutrinos, there are only mass square differences available, i.e. $\Delta m_{21}^2 = (m_\nu^2)^2 - (m_\nu^1)^2$ and $\Delta m_{32}^2 = (m_\nu^3)^2 - (m_\nu^2)^2$. Note that δ^{P} is not a directly observable quantity and has a large uncertainty, so it is not included in $\chi^2(\lambda)$. In conclusion, adopting the FN charge in Table II and $\lambda = 0.171$, our FN model could successfully explain 15 parameters in the standard model. In comparison, we also calculate the χ^2 by using the best three charge assignments in Table I of Ref. [20], and we find that our model has a smaller χ^2 .

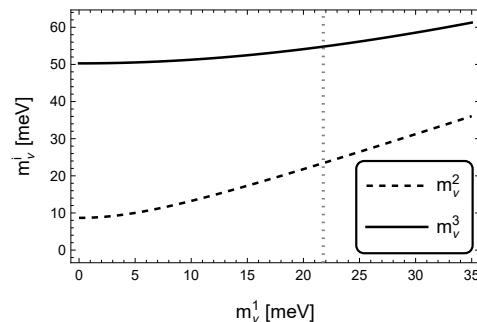


FIG. 5. Neutrino mass spectrum under the constraint from cosmology and oscillation measurements. The gray vertical dotted line indicates the upper bound on m_1 , above which the cosmological bound, i.e. Eq. (24), would be violated.

III. PREDICTIONS ON m_ν^i AND m_{ee}

In Sec. II, we have built a consistent FN model, and its predictions of 15 parameters agree very well with experimental observations. Based on this success, we are more interested in its predictions on the neutrino sector, especially, m_ν^i and m_{ee} . As we mentioned in Sec. II, the FN mechanism naturally prefers the NO. As a cross-check, we randomly generate a neutrino Yukawa matrix, y_ν , whose eigenvalues are $\{D_\nu^i\}$. If the average of $\{D_\nu^1, D_\nu^2, D_\nu^3\}$ is smaller than the median, y_ν is inverted order (IO). By sampling 10^6 times using our FN charge with $\lambda = 0.171$ and $\sigma = 0.3$, we find that NO takes up $\sim 98\%$. Therefore, we only consider NO in this work.

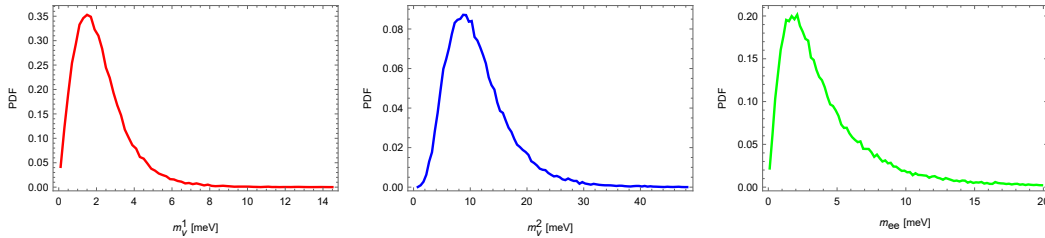


FIG. 6. The PDF of neutrino mass $m_\nu^{1,2}$ and effective Majorana mass element m_{ee} . Note that $m_3 = 0.05$ eV is adopted due to the cosmology and oscillation experiments constraints (see Fig. 5).

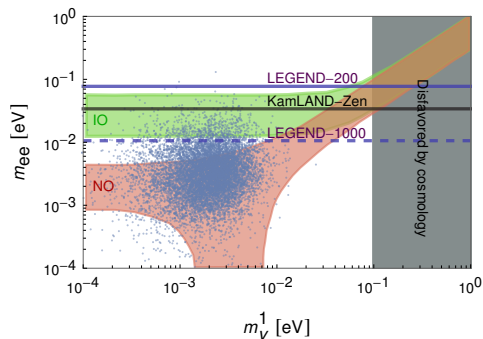


FIG. 7. The scattering plot (blue points) on m_ν^1 - m_{ee} plane with $\lambda = 0.171$ and $\sigma = 0.3$. The horizontal lines indicate different experiment constraints, e.g. KamLAND-Zen [33], LEGEND-200 [34], and LEGEND-1000 [25].

The neutrino oscillation experiments can tell the neutrino mass difference, e.g. Δm_{21}^2 and Δm_{32}^2 (see Table. I). Besides, the cosmology observations put constraints on total neutrino mass [31]

$$\sum_i m_\nu^i < 0.1 \text{ eV} . \quad (24)$$

Under these constraints, we can derive the neutrino mass spectrum (see Fig. 5). The x axis represents m_ν^1 , while the black dashed and solid lines represent m_ν^2 and m_ν^3 respectively. The vertical dotted line indicates the cosmological bound given by Eq. (24). One could see that m_ν^3 is almost a constant. Thus, we can take $m_\nu^3 = 0.05$ eV as a benchmark value to fix the neutrino mass normalization of our model. Specifically, by diagonalizing y_ν our model can predict m_ν^1/m_ν^3 and m_ν^2/m_ν^3 . After we fix m_ν^3 , we can get the PDF of m_ν^1 and m_ν^2 , which are shown in Fig. 6. It shows the most probable value of m_ν^1 and m_ν^2 are ~ 1.6 meV and ~ 9 meV respectively, which is perfectly consistent with Fig. 5.

As we mentioned the seesaw mechanism implies that the $0\nu\beta\beta$ process could happen. The decay rate is proportional to m_{ee}^2 , where m_{ee} measures the transition amplitude for an electron neutrino to an electron neutrino while violating the lepton number, which could be ex-

pressed as

$$m_{ee} = \left| \sum_i (U_{PMNS}^*)_{1i}^2 m_\nu^i \right| . \quad (25)$$

In the rightmost plot of Fig. 6 we demonstrate the PDF of m_{ee} . We find that most probable value of m_{ee} is located at $\sim 2 \times 10^{-3}$ eV, and m_{ee} is bounded by

$$0.503 \text{ meV} \lesssim m_{ee} \lesssim 18.0 \text{ meV} , \quad (26)$$

at 95% C.L.. Besides, in Fig. 7, we show the model prediction (blue dots) on the m_ν^1 - m_{ee} plane. The green and red regions represent the IO and NO cases, respectively. The gray region is excluded by cosmological observation [31]. Clearly, it shows most of the predictions overlap with the NO region. The near future $0\nu\beta\beta$ experiment LEGEND-1000 can check the validity of our model to some extent [25].

IV. SUMMARY AND DISCUSSION

In this short article, we propose a consistent FN model to deal with flavor puzzles and neutrino puzzles at the same time. One intriguing feature of this work is that we derive the FN charge of SM particles (see Table. II) by doing a qualitative analysis instead of a brutal search. Then, there is only one free parameter λ in our FN model, whose best value, i.e. $\lambda = 0.171$, is fixed through the minimum chi-square estimation. By randomly sampling g_{ij} , we calculate the PDFs of mass ratios, mixing angles, and CP angles (see Fig. 1 – Fig. 4). All these predictions agree with experimental observations quite well. We find that our charge assignments share some similarities with previous literature, e.g. Ref. [20], however, our FN model has a smaller $\chi^2(\lambda)$ and therefore fits the experimental observations better.

Another striking feature is that our model possesses a discrete \mathbf{Z}_{33} , which is anomaly-free and can be gauged. Unlike the global $U(1)_{FN}$ symmetry, the gauged \mathbf{Z}_{33} symmetry is free of quantum gravity corrections. Therefore, one could replace the $U(1)_{FN}$ with this gauged \mathbf{Z}_{33} , which makes our model more robust but would not change the existing conclusions.

Based on the success of our FN model, we also explore its prediction on the neutrino sector, especially, the value of m_ν^i and m_{ee} . We find that the FN mechanism naturally prefers the NO scenario, which is determined by its mathematical structure. Utilizing the neutrino oscillation and cosmology constraint, we calculate the mass spectrum in Fig. 5. It shows that m_ν^3 is almost a constant, i.e. $m_\nu^3 \sim 50$ meV. By adopting this benchmark value we predict that m_ν^1 and m_ν^2 are ~ 1.6 meV and ~ 9 meV respectively, which is perfectly consistent with the current observations. In addition, our model also gives a relatively precise constraint on m_{ee} , i.e. $0.503 \text{ meV} \lesssim m_{ee} \lesssim 18.0 \text{ meV}$ at 95% C.L. More interestingly, our model can be explored in a near future $0\nu\beta\beta$ experiment, such as LEGEND-1000 [25].

In Sec. II we introduce the factor \mathcal{N} to handle mass hierarchy between up-type quark and down-type quark and the charged lepton (see Eq. (2) and Eq. (9)). One possible origin of \mathcal{N} is that there are two different Higgs, like two-Higgs-doublet model [26] and supersymmetric theories at high energy. In fact, the FN charge could play the same role as \mathcal{N} , e.g. the λ^{c+f} in Eq. (4). For example, we find that if we reset $U(1)_{\text{FN}}^{dR} = \{3.5, 2.5, 2.5\}$,

$U(1)_{\text{FN}}^{eR} = \{6, 3, 2\}$, then \mathcal{N} is not necessary. However, the cost of this is that the discrete gauge symmetry \mathbf{Z}_{33} disappears.

The most distinguished feature of this work is the universality of the coupling g_{ij} (including the g'_{ij} for the neutrino sector). By combining this universality with the FN mechanism, we can successfully explain 15 SM parameters. Furthermore, its prediction on neutrino mass m_ν^i is surprisingly consistent with the current observation. Although the deep meaning behind this universality is unknown, we expect that there may be some hidden principles, and we save further explorations for future works.

ACKNOWLEDGMENTS

T. T. Y. is supported in part by the China Grant for Talent Scientific Start-Up Project and by Natural Science Foundation of China (NSFC) under grant No. 12175134 as well as by World Premier International Research Center Initiative (WPI Initiative), MEXT, Japan. Y. -C. Qiu thanks Kavli IPMU, U. Tokyo for its hospitality, where he finished this work.

-
- [1] G. Altarelli and F. Feruglio, “Discrete Flavor Symmetries and Models of Neutrino Mixing,” *Rev. Mod. Phys.* **82** (2010) 2701–2729, [arXiv:1002.0211 \[hep-ph\]](#).
- [2] H. Ishimori, T. Kobayashi, H. Ohki, Y. Shimizu, H. Okada, and M. Tanimoto, “Non-Abelian Discrete Symmetries in Particle Physics,” *Prog. Theor. Phys. Suppl.* **183** (2010) 1–163, [arXiv:1003.3552 \[hep-th\]](#).
- [3] D. Hernandez and A. Y. Smirnov, “Lepton mixing and discrete symmetries,” *Phys. Rev. D* **86** (2012) 053014, [arXiv:1204.0445 \[hep-ph\]](#).
- [4] S. F. King and C. Luhn, “Neutrino Mass and Mixing with Discrete Symmetry,” *Rept. Prog. Phys.* **76** (2013) 056201, [arXiv:1301.1340 \[hep-ph\]](#).
- [5] S. F. King, A. Merle, S. Morisi, Y. Shimizu, and M. Tanimoto, “Neutrino Mass and Mixing: from Theory to Experiment,” *New J. Phys.* **16** (2014) 045018, [arXiv:1402.4271 \[hep-ph\]](#).
- [6] S. F. King, “Unified Models of Neutrinos, Flavour and CP Violation,” *Prog. Part. Nucl. Phys.* **94** (2017) 217–256, [arXiv:1701.04413 \[hep-ph\]](#).
- [7] F. Feruglio and A. Romanino, “Lepton flavor symmetries,” *Rev. Mod. Phys.* **93** (2021) 015007, [arXiv:1912.06028 \[hep-ph\]](#).
- [8] W. Altmannshofer and J. Zupan, “Snowmass White Paper: Flavor Model Building,” in *Snowmass 2021*. 3, 2022, [arXiv:2203.07726 \[hep-ph\]](#).
- [9] **Super-Kamiokande** Collaboration, Y. Fukuda *et al.*, “Evidence for oscillation of atmospheric neutrinos,” *Phys. Rev. Lett.* **81** (1998) 1562–1567, [arXiv:hep-ex/9807003](#).
- [10] **SNO** Collaboration, Q. R. Ahmad *et al.*, “Direct evidence for neutrino flavor transformation from neutral current interactions in the Sudbury Neutrino Observatory,” *Phys. Rev. Lett.* **89** (2002) 011301, [arXiv:nucl-ex/0204008](#).
- [11] **Daya Bay** Collaboration, F. P. An *et al.*, “Observation of electron-antineutrino disappearance at Daya Bay,” *Phys. Rev. Lett.* **108** (2012) 171803, [arXiv:1203.1669 \[hep-ex\]](#).
- [12] P. Minkowski, “ $\mu \rightarrow e\gamma$ at a Rate of One Out of 10^9 Muon Decays?,” *Phys. Lett. B* **67** (1977) 421–428.
- [13] T. Yanagida, “Horizontal gauge symmetry and masses of neutrinos,” *Conf. Proc. C* **7902131** (1979) 95–99.
- [14] T. Yanagida, “Horizontal Symmetry and Mass of the Top Quark,” *Phys. Rev. D* **20** (1979) 2986.
- [15] M. Gell-Mann, P. Ramond, and R. Slansky, “Complex Spinors and Unified Theories,” *Conf. Proc. C* **790927** (1979) 315–321, [arXiv:1306.4669 \[hep-th\]](#).
- [16] C. D. Froggatt and H. B. Nielsen, “Hierarchy of Quark Masses, Cabibbo Angles and CP Violation,” *Nucl. Phys. B* **147** (1979) 277–298.
- [17] M. Leurer, Y. Nir, and N. Seiberg, “Mass matrix models: The Sequel,” *Nucl. Phys. B* **420** (1994) 468–504, [arXiv:hep-ph/9310320](#).
- [18] M. Leurer, Y. Nir, and N. Seiberg, “Mass matrix models,” *Nucl. Phys. B* **398** (1993) 319–342, [arXiv:hep-ph/9212278](#).
- [19] S. Nishimura, C. Miyao, and H. Otsuka, “Exploring the flavor structure of quarks and leptons with reinforcement learning,” [arXiv:2304.14176 \[hep-ph\]](#).
- [20] C. Cornella, D. Curtin, E. T. Neil, and J. O. Thompson, “Mapping and Probing Froggatt-Nielsen Solutions to the Quark Flavor Puzzle,” (6, 2023), [arXiv:2306.08026 \[hep-ph\]](#).
- [21] S. Weinberg, “Baryon and Lepton Nonconserving Processes,” *Phys. Rev. Lett.* **43** (1979) 1566–1570.
- [22] T. Yanagida, “NEUTRINO MASS AND

- HORIZONTAL SYMMETRY.,” in *1981 INS Symposium on Quark and Lepton Physics*. 1981.
- [23] **Particle Data Group** Collaboration, R. L. Workman *et al.*, “Review of Particle Physics,” *PTEP* **2022** (2022) 083C01.
- [24] **eBOSS** Collaboration, S. Alam *et al.*, “Completed SDSS-IV extended Baryon Oscillation Spectroscopic Survey: Cosmological implications from two decades of spectroscopic surveys at the Apache Point Observatory,” *Phys. Rev. D* **103** (2021) 083533, [arXiv:2007.08991 \[astro-ph.CO\]](#).
- [25] **LEGEND** Collaboration, N. Abgrall *et al.*, “The Large Enriched Germanium Experiment for Neutrinoless $\beta\beta$ Decay: LEGEND-1000 Preconceptual Design Report,” [arXiv:2107.11462 \[physics.ins-det\]](#).
- [26] G. C. Branco, P. M. Ferreira, L. Lavoura, M. N. Rebelo, M. Sher, and J. P. Silva, “Theory and phenomenology of two-Higgs-doublet models,” *Phys. Rept.* **516** (2012) 1–102, [arXiv:1106.0034 \[hep-ph\]](#).
- [27] L. Wolfenstein, “Parametrization of the Kobayashi-Maskawa Matrix,” *Phys. Rev. Lett.* **51** (1983) 1945.
- [28] M. Fedele, A. Mastroddi, and M. Valli, “Minimal Froggatt-Nielsen textures,” *JHEP* **03** (2021) 135, [arXiv:2009.05587 \[hep-ph\]](#).
- [29] G.-y. Huang and S. Zhou, “Precise Values of Running Quark and Lepton Masses in the Standard Model,” *Phys. Rev. D* **103** (2021) 016010, [arXiv:2009.04851 \[hep-ph\]](#).
- [30] S. P. Martin and D. G. Robertson, “Standard model parameters in the tadpole-free pure $\overline{\text{MS}}$ scheme,” *Phys. Rev. D* **100** (2019) 073004, [arXiv:1907.02500 \[hep-ph\]](#).
- [31] **Particle Data Group** Collaboration, R. L. Workman *et al.*, “Review of Particle Physics,” *PTEP* **2022** (2022) 083C01.
- [32] T. Banks and N. Seiberg, “Symmetries and Strings in Field Theory and Gravity,” *Phys. Rev. D* **83** (2011) 084019, [arXiv:1011.5120 \[hep-th\]](#).
- [33] **KamLAND-Zen** Collaboration, S. Abe *et al.*, “Search for the Majorana Nature of Neutrinos in the Inverted Mass Ordering Region with KamLAND-Zen,” *Phys. Rev. Lett.* **130** (2023) 051801, [arXiv:2203.02139 \[hep-ex\]](#).
- [34] **GERDA** Collaboration, M. Agostini *et al.*, “Final Results of GERDA on the Search for Neutrinoless Double- β Decay,” *Phys. Rev. Lett.* **125** (2020) 252502, [arXiv:2009.06079 \[nucl-ex\]](#).